2016 13th International Conference on Electrical Engineering, Computing Science and Automatic Control (CCE), Mexico, City. Mexico

Active Disturbance Rejection Control for Humanoid Stable Walking

S. M. Orozco-Soto, R. S. Núñez-Cruz and J. M. Ibarra-Zannatha
Robotics and Artificial Vision Laboratory
Automatic Control Department, CINVESTAV
Mexico City, Mexico
{sorozco, rnunez, jibarra}@ctrl.cinvestav.mx

***Abstract*—This paper presents an application of the active disturbance rejection control approach for humanoid robot stable walking, which is a control strategy based on the extended state observer and cascade integrator canonical form features from modern control theory to deal with disturbances, nonlinearities and unmodeled dynamics. The proposed controller is based on the 3D linear inverted pendulum walking pattern generation, and is designed to be triggered only if disturbance signals are detected. This control technique was tested on the model of a humanoid robot using numerical simulation software, showing successful results that motivate to implement it in a real humanoid robot platform.**

Keywords—humanoid robots; active disturbance rejection control; 3D linear inverted pendulum; stable walking

I. Introduction

Humanoid robots are developed to operate in environments already designed for humans and, inherently to the interaction with such environments, the robot suffers many kind of disturbances while walking like slip, pushes, dynamic parameter variations or unmodeled dynamics caused by object handling, or the pursuing of other complex activities. The walking tasks that humanoid robots perform consist, firstly, on the generation of stable walking patterns supplied to the robot and, then, optionally, the use a of a feedback stabilizer to ensure the correct execution of those walking patterns by means of disturbance rejection [1]. Several disturbance rejection techniques to guarantee humanoid stable walking have been developed and implemented successfully, [2-9], all these techniques requiring reference signals to operate and, most of them, demand an accurate dynamic model of the robot or a precise knowledge of the disturbance to be rejected, increasing the complexity of the control system design. A relatively recent control approach that allows real-time disturbance rejection that does not require an accurate dynamic model of the plant or a precise knowledge of the disturbance signals, is the active disturbance rejection control (ADRC), which is based in two of the best offerings of modern control theory: the canonical form representation and the state observer feedback control [10]. In this work, an ADRC is presented as a stabilizer for humanoid robot walking based on the 3D linear inverted pendulum (3D LIP) approach. This controller was chosen since it does not require an accurate dynamic model of the robot, it is capable to deal with a vast range of disturbances, and it can work without reference signals, keeping the 3D LIP based natural motion generation, and minimizing the use of the ankle joint torques, but only use them as control inputs if it is required in presence of disturbance signals. The proposed control system was tested on numerical simulation software using the model of a humanoid robot developed at our institution: *Johnny*, showing successful and motivating results. This paper is organized as follows: Section II presents an overview of ADRC. The humanoid robot *Johnny*, and its walking pattern generation are described in Section III. In section IV, the control system design is presented; in Section V, the numerical simulation results are shown, and finally, Section VI presents the concluding remarks.

II. Active Disturbance Rejection Control Approach

Active Disturbance Rejection Control (ADRC) is a control strategy that has become popular among control engineers and researchers, since it has the capability to deal with a vast range of uncertainties and disturbances with the advantages of easy implementation and energy savings [10]. The baseline of ADRC is the exploitation of two of the best offerings of modern control theory: the canonical form representation and the state observer [10]. Different control applications using ADRC have been implemented successfully [11], so that, it is motivating to implement this control approach in humanoid robots control.

A. ADRC general theoretical frame

Consider a dynamic system of the form:

$$\begin{aligned} \dot{x} &= f(t, x, u, w) \\ y &= h(t, x, u, w) \end{aligned} \tag{1}$$

Where $x \in \mathbb{R}^n$ is the state vector, $u \in \mathbb{R}^q$ is the control input, $f(x) \in \mathbb{R}^n$ is the dynamics vector and $h(x) \in \mathbb{R}^q$ is the output y, that comprises the variables to be analyzed [12]. Independently from its linear or nonlinear nature, the stated system (1) can be represented as a *cascade of integrators* canonical form under some conditions, like by means of a transformation $\dot{z} = T(x)$ as is presented below [12, 10]:

$$\begin{aligned} \dot{z}_1 &= z_2 \\ &\vdots \\ \dot{z}_{n-1} &= z_n \\ \dot{z}_n &= g(x, t, u, w) \\ y &= h(x) \end{aligned} \tag{2}$$

Notice that the dynamics of the system (1) include disturbances, parameter uncertainties and unmodeled dynamics in the vector w. Hence, considering $g(x, t, u, w)$ as a total

978-1-5090-3511-3/16/$31.00 ©2016 IEEE

disturbance, an Extended State Observer (ESO) for the system can be designed as follows [10]:

$$\begin{aligned} \dot{\hat{z}}_1 &= \hat{z}_2 - l_1(\hat{e}) \\ &\vdots \\ \dot{\hat{z}}_{n-1} &= \hat{z}_n - l_n(\hat{e}) \\ \dot{\hat{z}}_n &= -l_{n+1}(\hat{e}) + g(\hat{z}, t, u, w) \end{aligned} \tag{3}$$

Where $\hat{e} = \hat{z} - z$ and $l(\hat{e})$ is a vector function such that leads $\hat{z} \to z$ asymptotically. Then, the control law u can be computed by:

$$u = u_0(t, r, x) - K_0 \hat{z} \tag{4}$$

Where K_0 is the observer gain matrix and $u_0(t, r, \hat{x})$ is a controller that considers the return from the change of coordinates. The convergence of the state observer is demonstrated in [13].

B. Linear ADRC Overview

Now consider the following linear time invariant system:

$$\begin{aligned} \dot{x} &= Ax + Bu + Ew \\ y &= Cx \end{aligned} \tag{5}$$

Where $E \in \mathbb{R}^{n \times p}$ is the matrix that represents how the disturbance is distributed in each degree of freedom and $w \in \mathbb{R}^p$ is the disturbance signals vector, which is usually unknown but bounded. Recalling the central idea of ADRC that refers to use an ESO to estimate the unknown generalized disturbance [14], the following extended state representation using $\xi_1 = x, \xi_2 = \dot{x}$ and $\xi_3 = f(x, t, u, w)$ can be stated as follows:

$$\begin{aligned} \dot{\xi} &= A_e \xi + B_e u \\ y &= C_e \xi \end{aligned} \tag{6}$$

Where A_e, B_e are set into a controllable canonical form using a transformation $\xi = T(x)$. Notice that the matrix E disappears from equation (5) to equation (6), since its components are now part of the new extended model and are now included in A_e. Hence, the following state observer for (6) that leads $\hat{\xi} \to \xi$ is proposed:

$$\begin{aligned} \dot{\hat{\xi}} &= A_e \hat{\xi} + B_e u + L(y - \hat{y}) \\ \hat{y} &= C_e \xi \end{aligned} \tag{7}$$

Where $L \in \mathbb{R}^{n \times q}$ is the observer gain matrix. The observer gains are chosen using Hurwitz polynomials based on the observer bandwidth ω_0 to ensure the asymptotic stability of $A_e - LC_e$. Then, if the linear extended observer (LESO) is properly designed, the original plant is reduced to a cascade integrator system that may be effectively controlled with a linear state feedback control law with the form [11, 14]:

$$u = u_0 - K_0 \hat{\xi} \tag{8}$$

Where u_0 is the controller for the plant in the original coordinates.

III. The Humanoid Robot Plant

In order to test the proposed ADRC controller, the mathematical model of a real humanoid robot called *Johhny* was implemented; indeed, a 3D LIP approach for this robot with basis on the so called coarse-graining method is developed for walking control of this robotic system described below [1].

A. "Johnny" Humanoid Robot

The robotic plant *Johnny* consists in a humanoid robot with 22 DOF distributed as follows: 5 DOF in each leg, 3 DOF in each arm, a gripping DOF for each hand, 2 more DOF at the neck and, finally, a 2 DOF waist [15]. This humanoid robot was developed at the Laboratory within the Automatic Control Department, and it has been optimally designed using genetic techniques for mechanical design and local joints controllers considering the least possible energy consumption [16]. Furthermore, some walking pattern generators have been tested successfully using this robot, in addition to artificial vision works, like visual odometry [17], among other research activities.

B. 3D Linear Inverted Pendulum Model

Let the humanoid walking robot *Johnny* be approximated in 3D space as an imaginary linear inverted pendulum (LIP) as is displayed in Fig. 1, where it can be observed that such pendulum consists in the center of mass (CoM) of the robot attached to a massless prismatic joint that rotates freely about a supporting point that represents the ankle joint during the single support phase. The length of the prismatic joint can be modified using a kick force $f_k \in \mathbb{R}^3$; furthermore, consider a constraint plane $z = k_x x + k_y y + z_c$ that restricts the CoM to move along it; when the motion is horizontal, the slopes of the plane are $k_x = k_y = 0$. Then, the dynamics of the 3D LIP for horizontal motion is given by:

$$\begin{aligned} \ddot{x} &= \frac{g}{z_c} x + \frac{1}{m z_c} u_x \\ \ddot{y} &= \frac{g}{z_c} y + \frac{1}{m z_c} u_y \end{aligned} \tag{9}$$

Where g is the gravity acceleration, (x, y) is the CoM displacement coordinate and (u_x, u_y) are the control inputs that represents the *roll* and *pitch* ankle torques respectively. It is important to mention that the constant CoM height z_c is reached using local joints control, so that, the 3D LIP can be implementable. Hence, considering the state variables $x_1 = x$, $x_2 = \dot{x}$, $x_3 = y$ and $x_4 = \dot{y}$, the 3D LIP dynamics can be represented using the following state-space form:

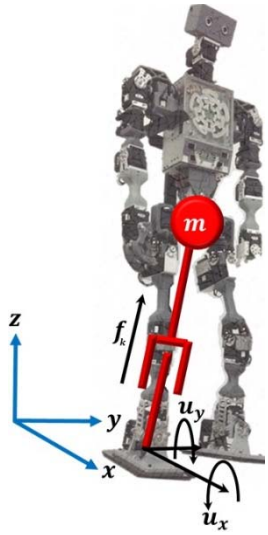

Fig. 1. Humanoid robot *Johnny* represented as a 3D LIP.

$$\dot{x} = Ax + Bu$$
$$y = Cx \tag{10}$$

Where:

$$A = \begin{bmatrix} 0 & 1 & 0 & 0 \\ \frac{g}{z_c} & 0 & 0 & 0 \\ 0 & 0 & 0 & 1 \\ 0 & 0 & \frac{g}{z_c} & 0 \end{bmatrix} \quad B = \begin{bmatrix} 0 & 0 \\ \frac{1}{mz_c} & 0 \\ 0 & 0 \\ 0 & \frac{1}{mz_c} \end{bmatrix}$$

$$C = \begin{bmatrix} 1 & 0 & 0 & 0 \\ 0 & 0 & 1 & 0 \end{bmatrix} \quad u = \begin{bmatrix} u_x \\ u_y \end{bmatrix}$$

Note that A is not Hurwitz and it has a saddle point equilibrium at $x = [0,0,0,0]^T$, which is the basis of the motion generation of the 3D LIP.

C. 3D LIP Based Humanoid Walking

In this section, the 3D LIP based walking pattern generation is presented.

Definition 1. A *walking primitive* is a piece of a 3D linear inverted pendulum trajectory, which is symmetric about y axis and defined in a period of $[T_0, T_{sup}]$ [1].

A walking primitive is depicted in Fig. 2, where its symmetry about y axis can be observed. Note that the motion starts in a time T_0 and ends in a time T_{sup}; in this interval, the motion in z is constant. Furthermore, the motion is performed from $(-\bar{x}, \bar{y})$ to $(\bar{x}, \bar{y})$. When the support time T_{sup} and the CoM height constraint z_c are defined, computing the walking primitive depends only on the terminal position $(\bar{x}, \bar{y})$, then, the terminal velocity for the n −th step can be obtained by [1]:

$$\bar{v}_x^{(n)} = \bar{x}(C+1)/T_c S \tag{11}$$

$$\bar{v}_y^{(n)} = \bar{y}(C-1)/T_c S \tag{12}$$

Where $T_c = \sqrt{z_c/g}$, $C = \cosh(T_{sup}/T_c)$ and $S = \sinh(T_{sup}/T_c)$. A set of walking primitives is called a *walking trajectory*; for each step of the humanoid walking trajectory, the following parameters must be computed to design a walking trajectory [1]:

$$\bar{x}^{(n)} = S_x^{(n+1)}/2 \tag{13}$$

$$\bar{y}^{(n)} = (-1)^n S_y^{(n+1)}/2 \tag{14}$$

Where $S_x^{(n+1)}$ is the length of the next step along the walking direction and $S_y^{(n+1)}$ is the step width for lateral direction, hence, the initial conditions for the n −th step walking primitive are:

$$\boldsymbol{x}_0^{(n)} = \left(-\bar{x}^{(n)}, \bar{v}_x^{(n)}, \bar{y}^{(n)}, -\bar{v}_y^{(n)}\right) \tag{15}$$

Finally, the foot placement is computed using:

$$\begin{bmatrix} p_x^{(n)} \\ p_y^{(n)} \end{bmatrix} = \begin{bmatrix} p_x^{(n-1)} \\ p_y^{(n-1)} \end{bmatrix} + \begin{bmatrix} \cos(S_\theta^{(n)}) & -\sin(S_\theta^{(n)}) \\ \sin(S_\theta^{(n)}) & \cos(S_\theta^{(n)}) \end{bmatrix} \begin{bmatrix} S_x^{(n)} \\ -(-1)^n S_y^{(n)} \end{bmatrix} \tag{16}$$

Where $\left(p_x^{(n)}, p_y^{(n)}\right)$ is the foot coordinate and $S_\theta^{(n)}$ is the direction angle; realize that the foot coordinate should be computed for the next step supporting leg. In Fig. 3, the parameters of the walking trajectory explained above are depicted; the rounded rectangles represent the foot of the humanoid and $p_n = \left(p_x^{(n)}, p_y^{(n)}\right)$ represents its position on xy plane; notice that the direction angle of each step is measured from x axis in counter clock-wise direction. A complete example walking trajectory compounded by 4 steps is shown in Fig. 4, where the change of support leg and the computed foot placement for each step are presented. Note that the CoM trajectory projected on the xy plane is continuous; in addition, the steps have the same lengths and there is not direction change.

Remark 1. In order to perform a continuous CoM trajectory, consider that the length of the steps are based on the size of the humanoid robot and, consequently, the size of its legs, furthermore.

Remark 2. The walking primitives only depend on the position and velocity initial conditions, since the 3D LIP motion is generated intrinsically by its unstable nature, so that, no control inputs supplied by the ankle joints are required, i.e. $u_x = 0 = u_y$ for the support foot in turn.

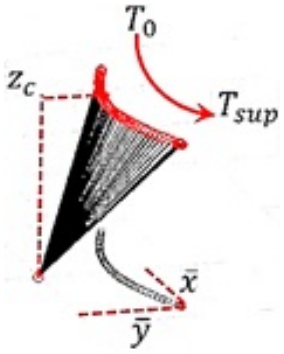

Fig. 2. Walking primitive.

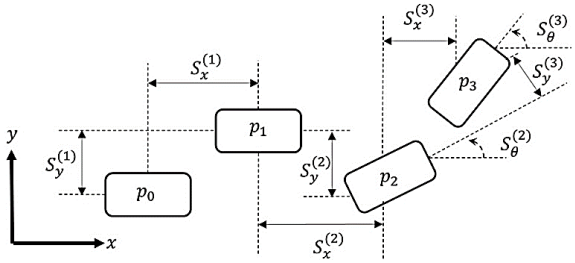

Fig. 3. Parameters of a walking trajectory.

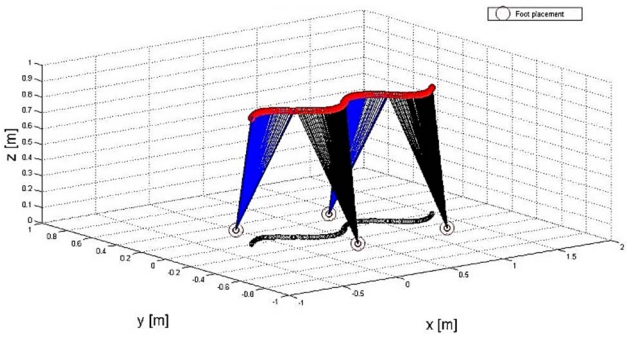

Fig. 4. Example of a walking trayectory.

IV. Control System Design

Regarding the disturbances that a humanoid robot suffers while walking in term of forces, its motion is affected by deviations from the nominal trajectory and from the horizontal constraint plane z_c [2]. Hence, the use of ankle joints torques as control inputs is proposed to compensate disturbances, liable to the following limitations.

A. Control Problems Formulation

Consider the humanoid robot *Johnny* modeled as a 3D LIP for walking control and remember that no control inputs supplied by the ankle joints are required provided that the robot performs a walking primitive designed with the initial conditions vector (15), then, the following control problems are stated:

a) Keep the control inputs of the supporting leg $u_x = 0 = u_y$ while no external disturbance is affecting the trajectory of the CoM of the humanoid robot. In other words, only in presence of an external disturbance, the control inputs must supply energy to reject it.

b) A robust feedback control would be a suitable solution if the desired trajectory of the CoM is known, however, it would increment the complexity of the control system since the desired trajectories and robust controllers must be designed and computing.

c) Since the ankle torques are limited in magnitude [2], a saturation function should be considered in order to limit the required control signal within the range of operation of the joints actuators.

In this work, an ADRC controller to deal with the control problems stated is considered as an appropriate solution, since only the ESO allows to only observe the disturbances and reject them if it is required, and furthermore, the need of a reference signal for the control design and operation can be left aside. Regarding the ESO based design of an ADRC, an extended state model was also developed for the later control system design.

B. Extended State Model of the Humanoid Robot

Consider the 3D LIP system (10). In order to design a suitable controller using ADRC approach, an extended state model of the form (6) was set up using the following state vector:

$$\xi = [x_1 \quad x_2 \quad x_3 \quad x_4 \quad w_x \quad w_y]^T \tag{17}$$

Where w_x and w_y are the disturbances affecting the motion in x and y direction respectively. Therefore, the extended state model matrices are:

$$A_e = \begin{bmatrix} 0 & 1 & 0 & 0 & 0 & 0 \\ \frac{g}{z_c} & 0 & 0 & 0 & 0 & 0 \\ 0 & 0 & 0 & 1 & 0 & 0 \\ 0 & 0 & \frac{g}{z_c} & 0 & 0 & 0 \\ 1 & 0 & 0 & 0 & 1 & 0 \\ 0 & 0 & 1 & 0 & 0 & 1 \end{bmatrix} \tag{18}$$

$$B_e = \begin{bmatrix} 0 & \frac{1}{mz_c} & 0 & 0 & 0 & 0 \\ 0 & 0 & 0 & \frac{1}{mz_c} & 0 & 0 \end{bmatrix}^T \tag{19}$$

$$C_e = I^{6\times 6} \tag{20}$$

Notice that the disturbances are an additional state and that affect directly the system dynamics. Since the system is now configured as an extended state model and is set up in a canonical form, a LESO can be designed to complete the disturbance rejection controller for humanoid stable walking.

C. Control System Design

A LESO of the form (7) is proposed for the on-line estimation of the disturbances affecting the humanoid robot walking, which gain matrix is given by:

$$L = \begin{bmatrix} l_{11} & l_{12} & 0 & 0 & l_{15} & 0 \\ l_{21} & l_{22} & 0 & 0 & 0 & 0 \\ 0 & 0 & l_{33} & l_{34} & 0 & l_{36} \\ 0 & 0 & l_{43} & l_{44} & 0 & 0 \\ 0 & 0 & 0 & 0 & l_{55} & 0 \\ 0 & 0 & 0 & 0 & 0 & l_{66} \end{bmatrix} \tag{21}$$

Where $l_{ij} \neq 0$ are positive constants based on the desired observer bandwidth. The state feedback control law that rejects the estimated disturbances:

$$u = \begin{bmatrix} \text{sat}(u_x) \\ \text{sat}(u_y) \end{bmatrix} = -\text{sat}\begin{bmatrix} 0 & 0 & 0 & 0 & K_{o_1} & 0 \\ 0 & 0 & 0 & 0 & 0 & K_{o_2} \end{bmatrix} \hat{\xi} \tag{22}$$

Where K_{o_1} and K_{o_1} are positive constants, and $\hat{\xi}$ is the estimated states vector. The bounds of the saturated functions for each component of the control input are determined independently according to the maximum torques of the motors actuating the joint. A block diagram of the control system is displayed in Fig. 5; observe that the reference input vector is 0, since only the initial conditions produce the motion; in addition, the saturation functions for the joint actuators limit the energy supplement. The controller block is the stabilizer for the humanoid robot closed-loop walking. Note that the observer

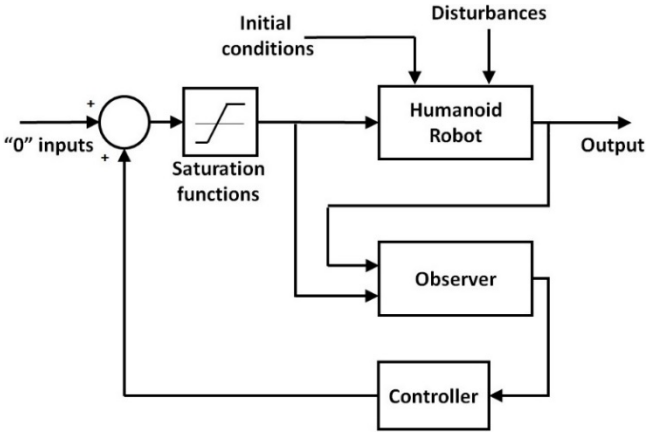

Fig. 5. Block diagram of the control system.

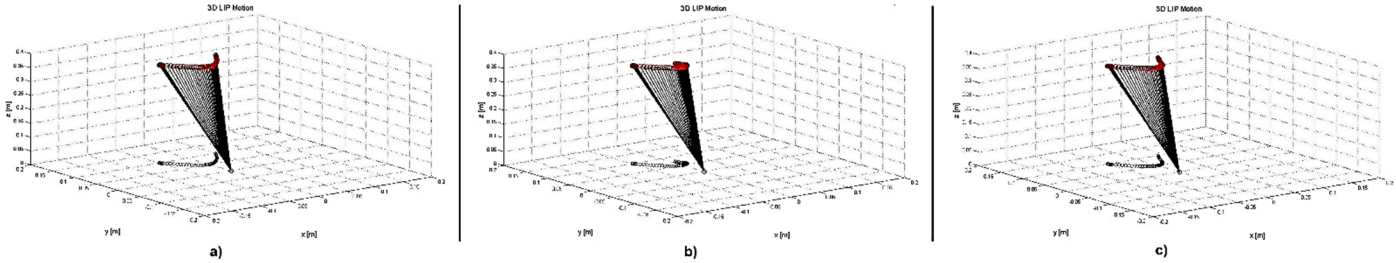

Fig. 6. Walking primitive performed a) Absence of disturbance b) Presence of disturbance and without control c) Presence of disturbance and with ADRC control.

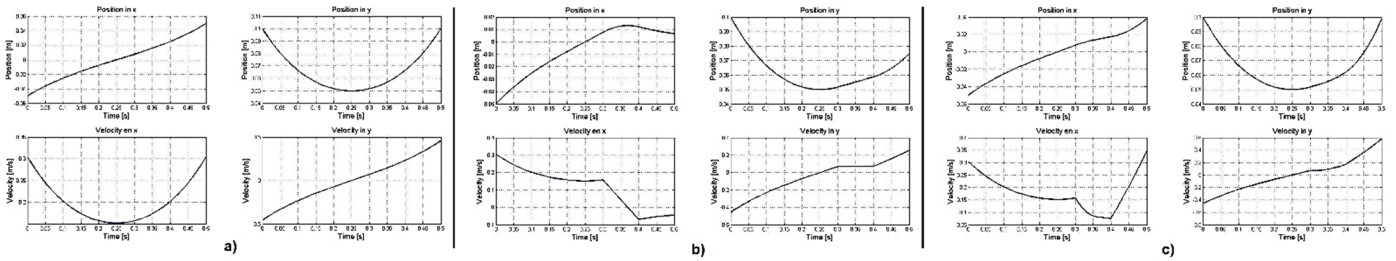

Fig. 7. Positions and velocities of the walking primitive a) Absence of disturbance b) Presence of disturbance and without control c) Presence of disturbance and with ADRC control.

V. RESULTS

The experiments to test the proposed ADRC for humanoid stable walking were performed using numerical simulation software. The parameters considering for the 3D LIP are listed in Table I; these parameters (except for gravity acceleration) were obtained using an optimal design approach [16]. The ADRC controller was tested in a single walking primitive with the parameters listed in Table II. The disturbance signal was modelling and implemented in simulation as a "push back" represented by a step input force against the direction of robot motion. In order to exemplify a disturbance situation, the following signal was used:

$$\begin{bmatrix} w_x \\ w_y \end{bmatrix} = \begin{bmatrix} f_d \cos(\delta) \\ f_d \sin(\delta) \end{bmatrix} \tag{23}$$

Where $f_d = -3\ [Nm]$ when $t \in [0.3 - 0.4][s]$, otherwise, $f_d = 0$. The considered angle was $\delta = 30°$. The observer matrix proposed that guarantees asymptotic convergence of the LESO is given by:

$$L = \begin{bmatrix} 15 & 27.79 & 0 & 0 & 1 & 0 \\ 1 & 30 & 0 & 0 & 0 & 0 \\ 0 & 0 & 15 & 27.29 & 0 & 1 \\ 0 & 0 & 1 & 30 & 0 & 0 \\ 0 & 0 & 0 & 0 & 13 & 0 \\ 0 & 0 & 0 & 0 & 0 & 13 \end{bmatrix} \tag{21}$$

The convergence of the LESO is guaranteed since $A_e - LC_e$ is Hurwitz, which is demonstrated with the computing of the eigenvalues presented below:

$$\text{eig}(A_e - LC_e) = \begin{cases} -22.4884 + 25.7428i \\ -22.4884 - 25.7428i \\ -12.0233 + 0.0001i \\ -22.4884 + 25.7428i \\ -22.4884 - 25.7428i \\ -12.0233 - 0.0001i \end{cases}$$

Notice that all eigenvalues have negative real part, hence, the convergence of the proposed LESO is demonstrated. A normal behavior of the 3D LIP motion in the Cartesian space is presented in Fig. 6a, this is a single walking primitive performed using the parameters of *Johnny*. The position and velocity about each axis during the walking primitive are depicted in Fig. 7a; notice that the positions and velocities are symmetric. Once the normal behavior of the 3D LIP is known, now the behavior under disturbance conditions will be analyzed. Consider the disturbance signals (23), if no control inputs are applied to the humanoid robot while the disturbances are applied during the walking primitive, the motion in Cartesian space is affected and the walking primitive is not executed correctly; such behavior is illustrated in Fig. 6b, where it can be observed that the walking primitive is not completed. Furthermore, in the position and velocity graphics displayed in Fig. 7b, it can be appreciated that position in x decreases, which means that the humanoid robot might fall backwards; in addition, tough position in y does not decrease, it also does not reach the target terminal position $\bar{y}$. The walking primitive displayed in Fig. 6c was executed with disturbances and implementing the ADRC technique. The position and velocity graphics of this motion are illustrated in Fig. 7c; observe that the positions do not decrease and they also evolve almost upon the target terminal values, which means that the controller rejected the disturbance signals and leading to a complete execution of the walking primitive. The control signals are shown in Fig. 8; it can be realized that they were triggered by the time the disturbance signals started, which means that only in presence of disturbances, the controller is triggered, as is suggested by the control problem *a)*. Furthermore, it can be observed that the control signal u_x reaches the value of 3.1 Nm, which is the maximum saturation value of the motor that actuates the *roll* joint of the ankle.

TABLE I. PARAMETERS OF THE 3D LIP.

PARAMETER	SYMBOL	VALUE	UNITS
TOTAL MASS OF THE ROBOT	m	4.39964	KG
RESTRICTED HEIGHT OF THE COM	z_c	0.35289	M
GRAVITY ACCELERATION	g	9.81	M/S^2

TABLE II. PARAMETERS OF THE WALKING PRIMITIVE.

PARAMETER	SYMBOL	VALUE	UNITS
SUPPORT TIME	T_{sup}	0.5	S
STEP LENGTH ALONG WALKING DIRECTION	S_x	0.05	M
LATERAL STEP LENGTH	S_y	9.81	M
DIRETION ANGLE	S_θ	0	°
INITIAL POSITION OF THE COM IN x	$\bar{x}_0$	0	M
INITIAL POSITION OF THE COM IN y	$\bar{y}_0$	0.1	M

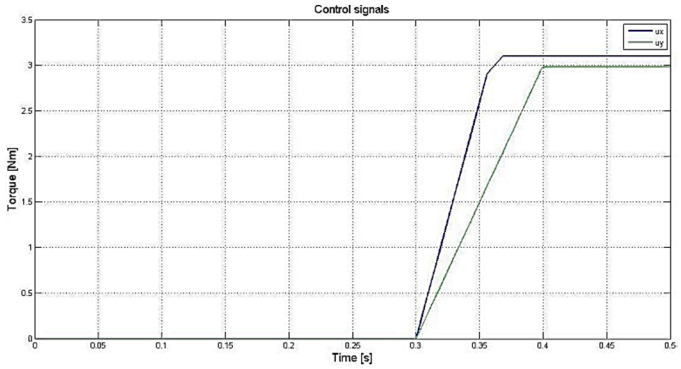

Fig. 8. Control signals computed by the proposed ADRC.

VI. CONCLUDING REMARKS

In this work, an alternative of disturbance rejection control system for stable humanoid robot walking using 3D LIP approach is presented. Some control problems were formulated for the correct functionality of the 3D LIP based humanoid walking, leading to the proposition of an ADRC strategy, since no control inputs from the ankle joints are required unless disturbance signals are detected and, in addition, no reference signal is either required to perform a walking primitive. The proposed controller was tested in numerical simulation software using an extended state 3D LIP based model of the humanoid robot *Johnny*, which was developed at our institution and is helpful for robotics, computer vision, control systems, among other research applications. The simulation results of the proposed control strategy shows that it is capable to handle successfully the control problems stated by triggering the control signals only in presence of disturbances in order to reject them, and, consequently, allowing the execution of walking primitives without the need of a reference signal. Furthermore, the control signals are saturated in order to keep them within the range of operation of the motors that actuate the ankle joints, preventing the actuators themselves and power electronics from damage. Although in this work, only push back-like disturbances were considered, ADRC have the potential to handle other kind of disturbances that humanoid robots suffers while walking, and that, in practice, such disturbances can be detected using the internal sensors of the robot such as the inertial measurement unit, force sensors at the feet, etc. The presented successful simulation results are the first steps on the development of robust control systems that ensure stable humanoid robot walking, therefore, further works in implementation of ADRC in other humanoid robot platforms and its comparison with alike control strategies are planned to be implemented.

REFERENCES

[1] S. Kajita, H. Hirukawa, K., Harada and K. Yokoi, "Introduction to humanoid robotics", Heidelberg: Springer, 2014

[2] S. Kajita and K. Tani, "Study of dynamic biped locomotion on rugged terrain-derivation and application of the linear inverted pendulum mode," in Proc. of Robotics and Automation, 1991 IEEE Int. conf. on, 1991, pp. 1405-1411.

[3] J. Morimoto, and C. G. Atkeson, "Robust low-torque biped walking using differential dynamic programming with a minimax criterion," in Proc. of Climbing and Walking Robots, 5th Int. conf. on, 2002, pp. 453-459.

[4] S. Hyong and G. Cheng, "Disturbance rejection for biped humanoids," in Proc. of Robotics and Automation, 2007 IEEE Int. conf. on, 2007, pp. 2668-2675.

[5] V. Prahlad, G. Dip, and C. Meng-Hwee, "Disturbance rejection by online ZMP compensation," in Robotica, vol. 26, no. 1, 2008, pp. 9-17.

[6] B. J. Stephens and C. G. Atkeson, "Push recovery by stepping for humanoid robots with force controlled joints," in Proc. of Humanoid Robots, 10th IEEE-RAS Int. conf. on, 2010, pp. 52-59.

[7] J. J. Alcaraz-Jiménez, M. Missura, H. Martínez-Barberá and S. Behnke, "Lateral disturbance rejection for the nao robot," in RoboCup 2012: Robot Soccer World Cup XVI, 2012, pp. 1-12.

[8] M. Kelly and A. Ruina, "On-linear robust control for inverted-pendulum 2D walking," in Proc. of Robotics and Automation, 2015 IEEE Int. conf. on., 2015, pp. 4353-4358.

[9] F. Hill and F. Fahimi, "Active disturbance rejection for walking bipedal robots using the acceleration of the upper limbs," in Robotica, vol. 33, no. 2, 2015, pp. 264-281.

[10] Y. Huang and W. Xue, "Active disturbance rejection control: methodology and theoretical analysis," in ISA transactions, vol. 53, no. 4, 2014, pp. 963-976.

[11] Q. Zheng and Z. Gao, "On practical applications of active disturbance rejection control," in Proc. of 29th IEEE Chinese control conf., 2010, pp. 6095-6100.

[12] H. K. Khalil, "Nonlinear systems," 3rd edition, Upper Saddle River, N.J: Prentice Hall, 2002.

[13] D. Yoo, S. S. T. Yau and Z. Gao, "On convergence of the linear extended state observer," in Proc. of Intelligent Control, 2006 IEEE Int. symp. on, 2006, pp. 1645-1650.

[14] W. Tan and C. Fu, "Linear Active Disturbance-Rejection Control: Analysis and Tuning via IMC," in IEEE Transactions on Industrial Electronics, vol. 63, no. 4, 2016, pp. 2350-2359.

[15] R. S. N. Cruz and J. M. I. Zannatha, "Johnny: desarrollo de un robot humanoide óptimo basado en caminantes dinámicos pasivos," in Proc. of XVI Mexican Robotics Cong. (COMRob), 2014.

[16] R. S. N. Cruz and J. M. I. Zannatha, "Optimal design for a humanoid robot based on passive dynamic walkers and genetic algorithms," in Proc. of Electrical Engineering, Computing Science and Automatic Control (CCE), 12th IEEE Int. conf. on, 2015, pp. 1-6.

[17] R. S. N. Cruz and J. M. I. Zannatha, "Inertial-visual odometry on mobile devices," on Proc. of Future Trends in Robotics, Open conf. on, 2016, pp. 121-128.